

Straightforward Micropatterning of Oligonucleotides in Microfluidics by Novel Spin-On ZrO₂ Surfaces

Gioia Della Giustina,^{†,‡} Alessandro Zambon,^{†,§} Francesco Lamberti,^{†,‡,§} Nicola Elvassore,^{†,‡,§} and Giovanna Brusatin^{*,†,‡}

[†]Department of Industrial Engineering, University of Padova, Via Marzolo 9, 35131 Padova, Italy

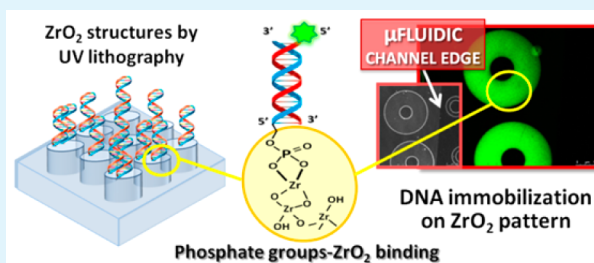
[‡]National Interuniversity Consortium of Materials Science and Technology (INSTM), Padova Research Unit, Via Marzolo 9, 35131 Padova, Italy

[§]Venetian Institute of Molecular Medicine (VIMM), Via Orus 2, 35129 Padova, Italy

S Supporting Information

ABSTRACT: DNA biochip assays often require immobilization of bioactive molecules on solid surfaces. A simple biofunctionalization protocol and precise spatial binding represent the two major challenges in order to obtain localized region specific biopatterns into lab-on-a-chip (LOC) systems. In this work, a simple strategy to anchor oligonucleotides on microstructured areas and integrate the biomolecules patterns within microfluidic channels is reported. A photosensitive ZrO₂ system is proposed as an advanced platform and versatile interface for specific positioning and oriented immobilization of phosphorylated DNA. ZrO₂ sol–gel structures were easily produced on fused silica by direct UV lithography, allowing a simple and fast patterning process with different geometries. A thermal treatment at 800 °C was performed to crystallize the structures and maximize the affinity of DNA to ZrO₂. Fluorescent DNA strands were selectively immobilized on the crystalline patterns inside polydimethylsiloxane (PDMS) microchannels, allowing high specificity and rapid hybridization kinetics. Hybridization tests confirmed the correct probe anchoring and the bioactivity retention, while denaturation experiments demonstrated the possibility of regenerating the surface.

KEYWORDS: hybrid material, sol–gel, optical lithography, DNA functionalization, microfluidic



INTRODUCTION

DNA based biochips for diagnostic assays and biosensor applications require immobilization of DNA strands on a solid surface.^{1–4} Technological advances also need a precise control of biomolecules binding sites with spatial positioning accuracy and well-defined area and geometries, in order to obtain localized region specific biopatterns;^{1,5–8} besides, their integration in microfluidic platforms is essential to develop fast, sensitive, and portable cheap diagnostic tools.^{9,10} They allow one to achieve high specificity and enhanced hybridization kinetics, as well.^{11,12} Therefore, simple strategies to immobilize and integrate biomolecules patterns in a microfluidic architecture would certainly advance diagnostic assay and biosensing techniques.

In this scenario, we aim to engineer a novel multiplex photosensitive crystalline ZrO₂ surface which is directly structured by lithography and can be easily incorporated into lab-on-a-chip (LOC) architectures; besides, the material structure engineering also provides a straightforward method to drive oligonucleotides binding with precise spatial control, without the need for complex substrate or biomolecule functionalization protocols. The novelty of the work relies on the simplified strategy to create region specific anchoring of

oligonucleotides on a wide variety of substrates (silicon, glass, gold), with respect to current procedures:^{7,13–17} for the first time, a spin-on ZrO₂ photosensitive material that can be directly patterned and easily integrated in microfluidic platforms is converted to a crystalline ZrO₂ interface with maximized affinity to oligonucleotides anchoring in a straightforward procedure.

First of all, the reported results show that the resist like behavior of the designed spin-on ZrO₂ system does not require multistep patterning processes such as those in traditional photolithographic patterning including the chemical etching¹⁸ or long-lasting protocols used to properly modify the surfaces in some local photoactivation method.^{19,20} On the other hand, some of the main limitations of widespread technologies for oligonucleotide positioning and micropattern fabrication, such as automated microspotting, microcontact printing,^{21,22} or Dip-Pen lithography,²³ are overcome with the presented strategy, with particular regard to their high cost, low accuracy of

Received: February 3, 2015

Accepted: May 27, 2015

Published: May 27, 2015

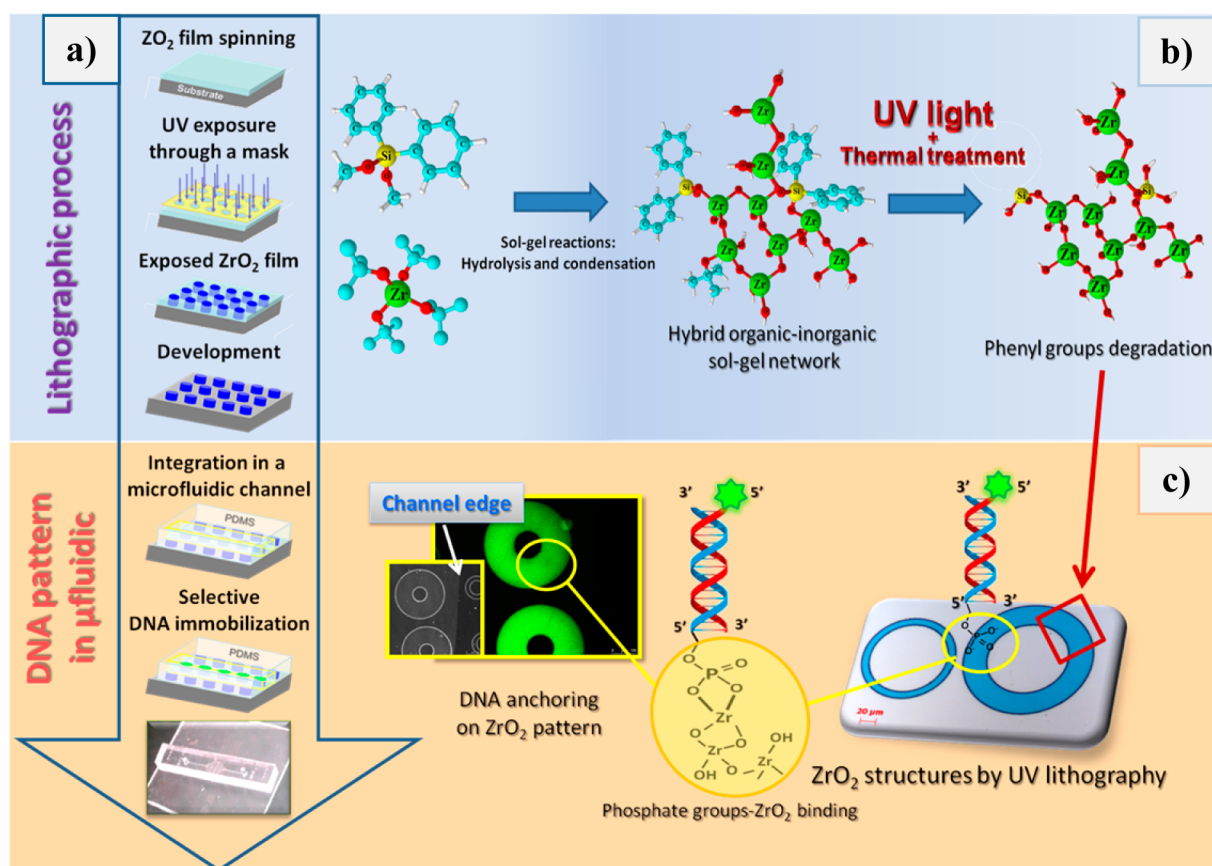


Figure 1. Immobilization of 5' phosphorylated DNA on ZrO_2 patterns integrated in the microfluidic channel: (a) Overview of the whole process: UV lithography, pattern integration in a microfluidic channel, and anchoring of fluorescent DNA strands (see Experimental Section for details). (b) Schematic illustration of ZrO_2 material synthesis and structural evolution during UV exposure, patterning, and thermal curing. (c) Optical microscopy of fluorescent oligonucleotides strands patterns and scheme of the chemical interaction between the terminal phosphate groups of the immobilized probe and ZrO_2 micropatterns.

positioning, small area covering, and low robustness in the case of microcontact printing.^{24,25}

A second issue concerns the characteristics of the engineered photosensitive ZrO_2 material, which allows one to exploit a functionalization protocol based on phosphate groups and the Zr surface chemistry, already described in the literature;^{4,7,26,27} generally, the reported materials, sometimes made by the sol-gel route, are not photosensitive or require multistep depositions. Our approach offers a straightforward functionalization method with respect to some of the current biografting procedures.

In fact, several immobilization protocols to anchor and position oligonucleotides on solid supports have been reported. Usually, different types of substrates (glass, silicon, gold, plastic, and so on) required the development of customized immobilization protocols, according to their surface chemistry.^{13,28–30} Self-assembled monolayers (SAMs) and layer by layer (LbL) techniques play a central role in this field since they connect inorganic materials (e.g., glass or silicon that are often used in these platforms) and the biological molecules of interest. Examples are DNA functionalization through the well-established reaction between *N*-hydroxysuccinimide (NHS) ester groups and an amino functionality of Amino($-NH_2$) modified DNA,^{14,18,31} surface silanization by organosilane modification of glass, gold, and metal oxides substrates^{32,33} or biotinylated-modified surfaces,^{34,35} and zirconium phosphate/phosphonate multilayer strategies.^{7,36,37}

All the above approaches for biomolecules anchoring envisage multistep and complex protocols. Avoiding time-consuming procedures and all the problems related to the achievement of well ordered and good quality SAMs and LbL depositions is highly desirable.

Herein, we present an innovative and simple approach to oriented biomolecules immobilization and patterning in microfluidic channels (Figure 1), by using a negative tone spin-on ZrO_2 based sol-gel photosensitive system. The material was chemically designed (i) to directly pattern inorganic ZrO_2 microstructures by photolithography (Figure 1a,b): organic functionalities are introduced in the inorganic network as photosensitive elements;³⁸ (ii) to engineer the surface chemistry of the sol-gel platform for specific and direct immobilization of DNA molecules without any modification. This outcome was achieved thanks to the naturally occurring terminal 5'-phosphate groups in DNA strands (Figure 1c) and exploiting the surface specificity and affinity between the Zr atoms and phosphate groups.^{4,7,26,27} To the best of our knowledge, the use of a spin-on ZrO_2 material, which can be both patterned and functionalized in a direct and straightforward process with different oligonucleotides and is easily integrated in the microfluidic platform, has been investigated and demonstrated for the first time.

Table 1. ssDNA Sequences Used in Immobilization Experiments and during the DNA–DNA Hybridization Tests

DNA denomination	base sequence (5'–3')	5' modification
probe 1	GGGCAGGCCATTCTCCTTCA	phosphate group
FCT (full complementary target)	TGAAGGAGGAATGGCCTGCC	fluorescein labeled
NCT (noncomplementary target)	ACTTCTCCTTACCGGACGGG	Alexa 594 labeled
probe 2	CCCGTCCGGTAAGGAGGAAGT	phosphate group

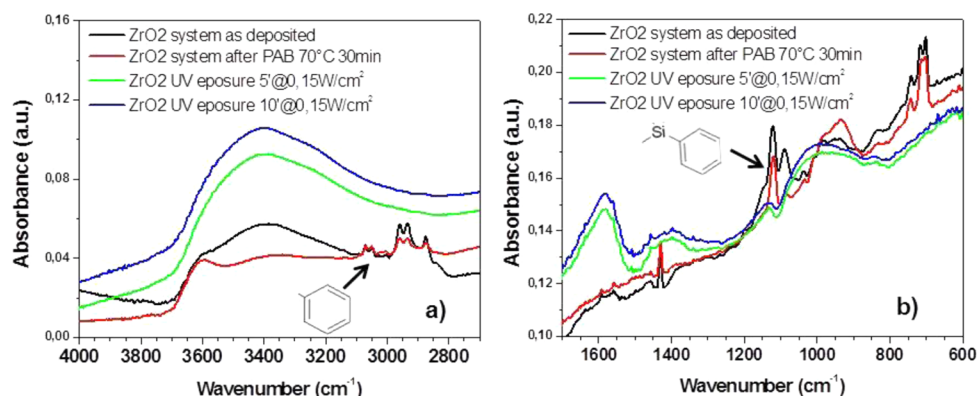


Figure 2. FT-IR spectra of ZrO₂ sol-gel film, deposited on Si, in a range between (a) 4000–2700 cm⁻¹ and (b) 1700–600 cm⁻¹ after the PAB thermal treatment and exposed to increasing UV doses.

EXPERIMENTAL SECTION

Synthesis of ZrO₂ Based System. A hybrid organic inorganic (HOI) SiO₂–ZrO₂ system was prepared by a sol-gel process through hydrolysis and condensation of an organically modified silicon alkoxide and a Zr alkoxide. All the reagents were purchased from Aldrich and used without further purification.

Zirconium butoxide (ZrBut) was mixed with methoxyethanol and stirred for 15 min at RT. Diphenyldimethoxysilane (DPhDMS) was then added to the sol (molar ratio ZrBut/DPhDMS = 8:2), and the solution was placed at 80 °C for 1 h. As a result, the synthesized system is made by a three-dimensional inorganic network of mixed bonds (Zr–O–Zr, Si–O–Si, and Zr–O–Si) with pendant organic phenyl groups that act as network modifier and sensitive elements (Figure 1b).

The final sol concentration was set between 120 and 25 g/L (SiO₂ + ZrO₂) according to the required thickness (Figure S1, Supporting Information). The solution was filtered by a microporous membrane (0.2 μm Millipore) in order to remove big particles improving the resist spin-coating quality. Moreover, the sol remains stable for up to 6 months even in the most concentrated condition.

HOI films, with suitable thickness, were deposited by spin coating on silicon wafer (orientation 100, from Si-Mat), soda lime glass (from Thermo Scientific), and fused silica slides (from Heraeus). No adhesion problems were displayed for these substrates. A post application-bake (PAB) in a forced air oven at 70 °C for 30 min was made to remove residual solvent. Thicknesses in the range between 600 and 50 nm were obtained (Figure S1, Supporting Information), with good optical quality and no pinhole or cracking formation.

Lithographic Process. The realization of microstructures was performed by using a Hamamatsu LC5 HgXe UV spot light source enhanced in the deep UV (250 nm band) with a power density of 150 mW/cm² on the sample surface. The scheme of the process is reported in Figure 1a,b. In particular, ZrO₂ spin-coated films were exposed in air using a quartz chromium mask with different patterns (features resolution between 2 and 100 μm). The optimum nominal UV dose depends on the features resolution and on the substrate used (Si or glass), because of the different amount of radiation reflected at the interface. On silicon, the exposure dose varies between 27 and 54 J/cm² (3–6 min), while a greater UV illumination (up to 9 min; 1.5× Si dose) is necessary on fused silica and soda lime glass substrates. Usually, higher resolution patterns require lower UV dose. After

exposure, a postexposure bake (PEB) at 100 °C for 30 s was made to increase the film contrast. Development in 3N HCl for 10–60 s, rinsing in water, and drying in nitrogen followed the PEB. Patterned films were treated at 150, 300, 500, or 800 °C for 30 min to promote the condensation reactions or modify the materials structure (inorganic-amorphous ⇒ crystalline), before microfluidic integration and DNA immobilization.

Microfluidic Integration and Oligonucleotides Immobilization. Polydimethylsiloxane (PDMS, Sylgard 184 Dow Corning) was used for replica molding in the ratio of 10:1 (base/cure agent). The mold was fabricated on a silicon wafer (Siebert DE) with 100 μm SU82100 (Microchem USA) with a circular geometry as previous reported.³⁹ The PDMS channels have been bound to fused silica substrates, both treated with UV-ozone plasma cleaner (Bioforce Nanosciences) for 15 min. The coupled chip was placed at RT for at least 12 h before performing experiments. Prior to UV-ozone treatment, the glass substrate was cleaned by rinsing with acetone (Sigma-Aldrich), methanol (Sigma-Aldrich), and distilled water, then dried with compressed air, and placed at 100 °C for at least 10 min before the insertion into the UV-ozone machine. The bonding and surface cleaning after UV-ozone treatment was tested and optimized as reported in Figures S2 and S3, Supporting Information. Microfluidic channels (1 μL volume) were pretreated with a commercial DNase removing solution and then rinsed with distilled water-DNase free.

A single-stranded DNA (ssDNA) probe was used at the concentration of 1 μM (phosphate-buffered saline (PBS), 1×, pH 7.4, Invitrogen) and incubated in the microfluidic channel at room temperature for 1 h. The fluorescent target solution (1 μM concentration) was incubated for 30 min in the dark and room temperature. The channel was then washed with distilled water RNase free for removing adsorbed species, before the characterization (Figure 1a,c). The oligonucleotide strands HPLC-purified by Invitrogen before use are reported in Table 1 (melting temperatures are listed in Table S1, Supporting Information).

Characterization Methods. A FEI Nova600i dual beam system with an electron acceleration voltage of 30 kV, equipped with an ultrahigh resolution field emission scanning electron microscopy (SEM), was used to characterize the patterned structures.

Fourier transform infrared spectroscopy (FTIR) was carried out using a Jasco FT-IR 620 spectrometer to follow the evolution of hybrid ZrO₂ system with thermal treatments (150, 500, and 800 °C). The analysis was performed within the 400–4000 cm⁻¹ range, with a 4 cm⁻¹ resolution for a total of 32 scans.

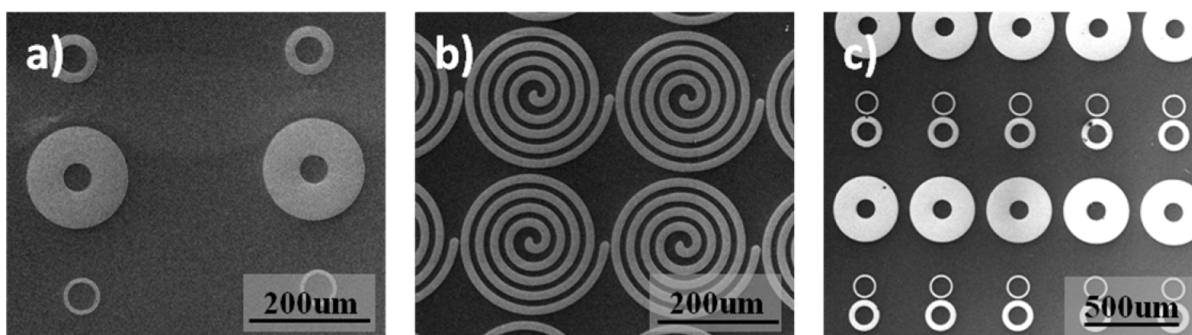


Figure 3. Examples of ZrO_2 sol-gel microstructures obtained by direct UV lithography. The 100 g/L ZrO_2 sol was spin coated on silicon at 2000 rpm \times 30 s, and the films were UV exposed for (a) 5 min, (b) 4 min, and (c) 6 min.

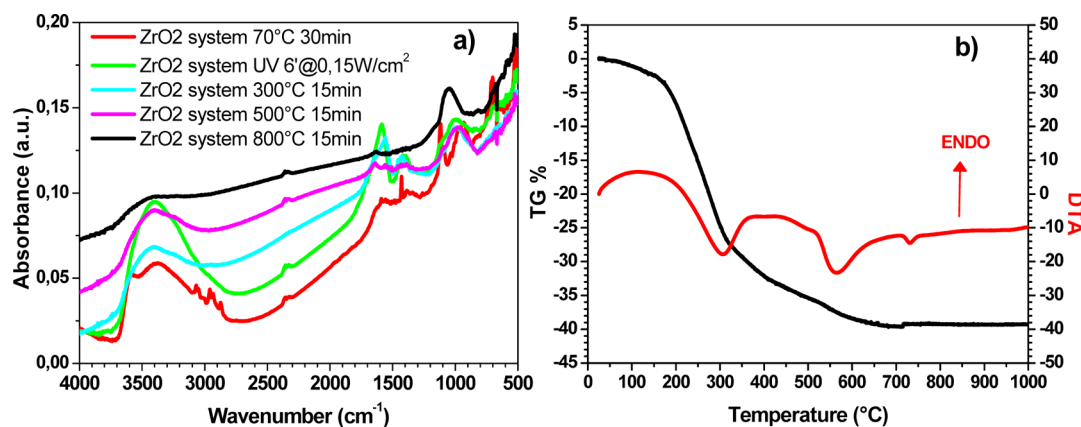


Figure 4. (a) FT-IR spectra of ZrO_2 sol-gel film deposited on Si, after thermal treatment at increasing temperatures. (b) TG and DTA analyses of ZrO_2 powders, performed in air.

Ellipsometric measurements (V-Vase J.A.Woollam Spectroscopic Ellipsometer) were performed to evaluate the vertical shrinkage of annealed ZrO_2 films (500 and 800 °C). Crystalline phases were identified by X-ray diffraction (XRD) measurements using a Philips diffractometer (Philips PW 1729) equipped with a Ni-filtered Cu K α radiation source. XRD spectra were recorded in Bragg-Brentano ω - 2θ geometry for thin film configuration.

Imaging was detected using an inverted fluorescence microscope Leica DMI6000B equipped with a mercury short-arc reflector lamp (Leica, Germany) excitation filters BP 450–490 nm with emission LP 515 (emission in green) and BP 515–560 nm with LP 590 (emission in red).

RESULTS AND DISCUSSION

ZrO_2 Pattern Realization. ZrO_2 patterned structures were prepared in a fast and simple direct route, by using a conventional UV lithography.³⁸ The structural changes undergone during the lithographic process were studied and reported in Figure 2. In particular, the effects of PAB and UV exposure on the film were monitored by FTIR spectroscopy, looking at the evolution of the phenyl groups upon exposure at increasing UV doses. Degradation of the aromatic rings proceeds with UV irradiation; this is clearly revealed by the disappearance of the two characteristic doublet peaks at 3070–3040 cm^{-1} due to the aromatic C–H stretching vibration in the diphenyl silica precursor.

The relative decrease in intensity of the band at 1460 cm^{-1} due to C–H bending and the absorption at 1120 cm^{-1} ascribed to the stretching of phenyl-silicon bond confirms the photodecomposition of aromatic moieties. Further structure modification during exposure can be revealed observing the

absorption bands in the region between 2700 and 2970 cm^{-1} : these peaks are due to the aliphatic C–H symmetric and asymmetric stretching vibrations in Si and Zr alkoxides, indicating the presence of a large amount of unreacted species (methoxy and butoxy groups) in the unexposed film. The mild PAB thermal treatment (30 min at 70 °C) promotes a slight hydrolysis of alkoxides substituents and an evident OH groups condensation progress (band between 3100 and 3700 cm^{-1}). UV light exposure is more efficient in promoting the complete hydrolysis of unreacted species as confirmed by the disappearance of the peaks related to the alkoxide groups. A concomitant consequence is the strong increment of the OH absorption band with increasing doses. This can be due to the formation of hydrolyzed Si–OH groups, also visible from the small band at 960–910 cm^{-1} , but it can be mostly due to the photodecomposition of aromatic rings with the development of silanol and molecular water, absorbing at 1640 cm^{-1} . The overall outcome is a different film structure in the exposed area, where the complete removal of the organic component and a progress of the inorganic network cross-linking is obtained. Moreover, OH groups, arising from hydrolyzed or photo-degraded species, are present inside the film structure and on the surface, and both species contribute to the formation of an OH band in the FT-IR spectra.

The changes induced by the UV irradiation are used to pattern the ZrO_2 by UV lithography. Films were exposed to UV light through a quartz mask having several test patterns. The exposed areas become almost completely inorganic, and a solubility change occurs compared to the unexposed one. A negative resist like behavior allows the unirradiated areas of the

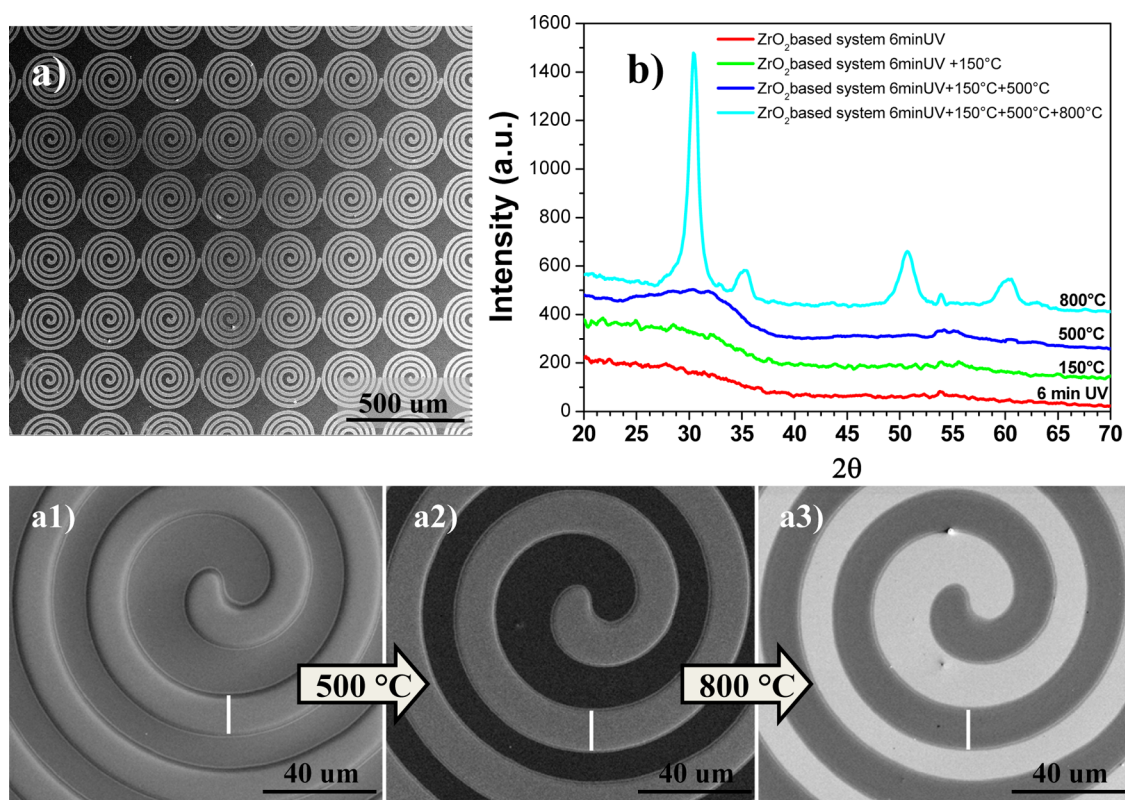


Figure 5. (a) SEM images of ZrO₂ structures obtained by UV lithography. Magnification of a pattern thermal treated at (a1) 150 °C for 30 min, (a2) 500 °C for 30 min, and (a3) 800 °C for 30 min. The same sample was used for the consecutive thermal treatments and almost no lateral contraction occurred with increasing temperature (see vertical marker). (b) XRD spectra of the same sample exposed to UV light and heated at increasing temperatures (150, 500, and 800 °C for 30 min).

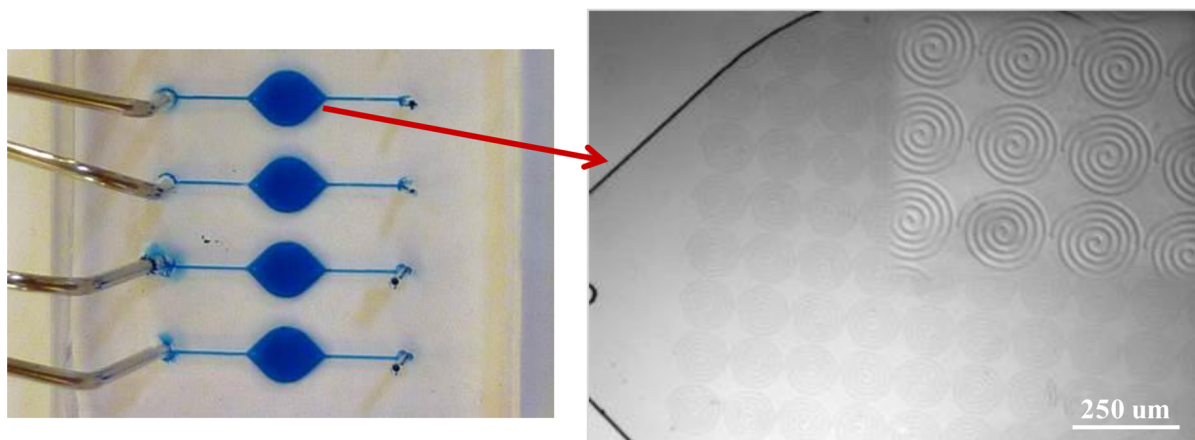


Figure 6. Optical microscopy of ZrO₂ based pattern obtained by UV lithography on fused silica, treated at 500 °C and integrated in a microfluidic channel (100 μm height, 1 μL volume, left). On the right, a magnification of the ZrO₂ structures.

film in acidic solution to dissolve. The microstructures, reported in Figure 3, were obtained with different doses (according to the pattern resolution) and a development time of 35 s in 3 N HCl, after a PEB of 30 s at 100 °C.

A fully cross-linked crystalline ZrO₂ film is necessary for a higher affinity of DNA respect to amorphous ZrO₂, as reported in ref 38, and can be achieved by proper thermal treatments after UV exposure. Therefore, films treated at different temperatures were characterized. As shown in the FT-IR spectra (Figure 4a), a broad band around 950–940 cm⁻¹ due to mixed Zr–O–Si bonds overlapped with the contribution related to the Si–OH species is clearly visible until 500 °C.

The decrease in intensity of the OH band is observed only after thermal treatment at 800 °C, with a simultaneous crystallization of the ZrO₂ film in the tetragonal system.^{38,40} The absorption peak at 1175 cm⁻¹ is due to the growth of thermal SiO₂ promoted by the high temperature treatment.

Dimensional Stability of Pattern and Microfluidic Integration. As shown by XRD measurements of UV exposed films treated at different temperatures (Figure 5b), ZrO₂ crystallization in the tetragonal phase is achieved at 800 °C. This is an important step since DNA shows higher affinity to crystalline patterns with respect to the amorphous ones.³⁸

However, the dimensional stability of the patterned features is a critical issue in micro and nano fabrication processes. The formulation of our ZrO_2 system was engineered to prevent lateral shrinkage during treatments at high temperatures. Figure 5 shows SEM analyses of the same UV patterned geometries tested at growing temperatures (Figure 5a1,a2,a3): by SEM inspection, the microstructures do not present any visible defects or cracking. In spite of a vertical shrinkage of about 41% at 500 °C and 47% at 800 °C, the lateral shrinkage is within 5% with respect to the initial size even after heating at high temperatures. Therefore, the thermal treatment at high temperature, necessary to obtain crystalline patterns with high DNA affinity, can be performed without affecting the lateral features size.

The crystalline ZrO_2 patterns have been coupled with a microfluidic circuit. In this way, the hybridization assay can be controlled by a double spatial constraint, imposed by the patterned substrate and the microfluidic channel. An example of integration of crystalline ZrO_2 microstructure in a microfluidic platform is reported in Figure 6. PDMS channels and fused silica patterned substrate can be easily bonded and irreversibly sealed. Flow tests have demonstrated a sealing resistance of channels up to 3 bar, after the UV ozone process (see the Supporting Information, Figure S2).

Biofunctionalization with DNA and DNA–DNA Hybridization Tests in Microfluidic. The bioaffinity of patterned crystalline ZrO_2 substrates was tested in a microfluidic architecture by using fluorescent complementary DNA strands. In particular, the experiments were performed by using a 21-base pair terminal phosphorylated DNA probe (Probe 1). An evident fluorescence, with an emission maximum at 520 nm, was revealed just on the patterned areas inside the channel (Figure 7a). No fluorescent intensity was detected outside the channels. The fluorescent emission due to hybridization of fluorescein labeled full complementary target (FCT) reveals the correct binding and accessibility of the probe. The presence of terminal phosphate group allows an oriented anchoring with a

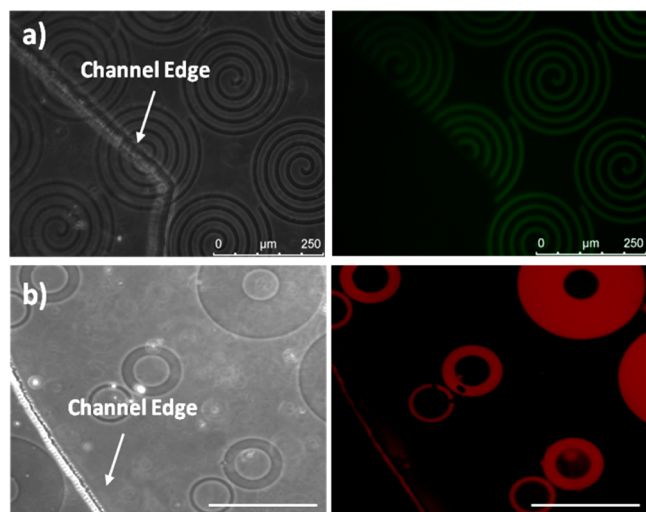


Figure 7. BF micrograph (sx) and fluorescent (dx) image of ZrO_2 features thermally treated at 800 °C and functionalized with Probe 1 for 1 h and incubated with the complementary FCT strand for 30 min (a) and Probe 2 with its complementary NCT strand (b) in a microfluidic channel. No fluorescence was revealed outside the channel. White arrow indicates the edge of the microfluidic channel. Scale bar is 250 μm .

perpendicular configuration which enables the probe to freely hybridize. NCT was also used as negative control and left to interact with probe 1 for 30 min: no fluorescent signal was detected, confirming the absence of nonspecific absorption. Analogous results were achieved with probe 2 and its complementary strand NCT (see Figure 7b). This outcome is justified by the surface specificity of zirconium oxide for the 5'-phosphate of DNA, as in the case of zirconium phosphonate and phosphate arrays.^{27,36,37}

In particular, phosphate anions and monosubstituted phosphates groups tend to bind to the crystalline metal oxide surface mainly in a “bidentate” mode,⁴¹ similarly to many chelating agents such as carboxylic acids. In fact, the Zr surface atoms, that have fewer nearest neighbors than the corresponding ions in the bulk, are coordinatively unsaturated. Therefore, the surface states promote a coordinate covalent bond as it is often exploited in metal oxide affinity chromatography (MOAC) for the enrichment of phosphopeptides.⁴² This bioaffinity is a key point to target DNA and DNA–protein with no need of further chemical modifications of substrates and DNA or proteins. In fact, the phosphate group naturally occurs in human DNA and chemical modification of terminal probe strands with this functionality is routinely achieved using enzymatic (T4 polynucleotide kinase) or chemical (phosphoramidite chemistry) routes.³⁷ However, two critical issues for the development of a sensor device or DNA recognition assay are nonspecific absorption and reproducibility.^{43,44}

Hence, after demonstrating a successful anchoring, the nonspecific absorption was verified. In fact, the presence of a negatively charged phosphate ester backbone could induce interaction of the DNA strands with the ZrO_2 surface through these groups, leading to a horizontally tilted conformation. This nonspecific DNA bonding would reduce the availability of DNA probe for hybridization, and it has to be avoided in order to enhance the hybridization efficiency. Equally, the nonspecific absorption of labeled complementary target should be prevented to minimize the background intensity and improve the signal to the noise ratio.

Fluorescently labeled ssDNA strands (FCT and NCT) without the terminal phosphate moiety have been used to investigate the nonspecific attachment on the ZrO_2 surface. The nonphosphate-functionalized oligonucleotide sol (1 μM) has been deposited onto the crystalline patterned features and left to interact for 1 h at RT. The fluorescence analyses did not show any signal (see the Supporting Information, Figure S4), and only at high exposure time, a slight autofluorescence of the material can be revealed. This result reasonably indicates that no detectable DNA strands have been absorbed on the patterned features through phosphate ester backbone and supports the specificity of phosphorylated DNA strands to the ZrO_2 surface. The affinity of terminal phosphate moiety is due to its higher basicity and the existence of at least two anchoring points. This brings the DNA to prefer a coordination binding through the free phosphate functionality, assuming a perpendicular conformation, which in turn facilitates hybridization.

To explain the specific interaction between phosphorylated DNA and ZrO_2 films, it has been taken into account that the surface charge of Zr oxide and DNA can be affected by pH. A n -mer DNA contains $n - 1$ negative charges from the backbone phosphate whose pK_a value is around 2. Within the pH range from 5 to 8, the bases are noncharged⁴⁵ and therefore DNA is highly negatively charged at neutral pH thanks to the phosphate functionalities. This condition makes the surface

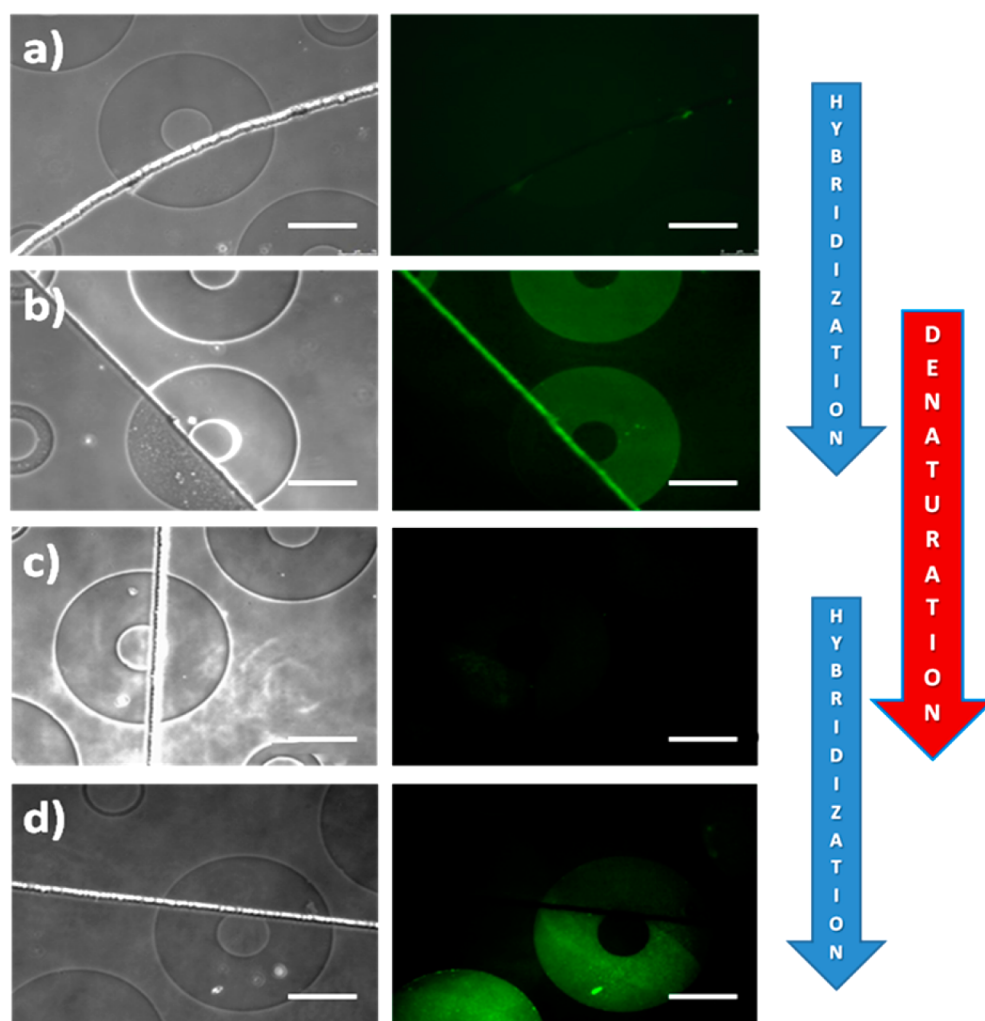


Figure 8. Optical microscopies and fluorescent images of ZrO_2 features thermally treated at $800\text{ }^\circ\text{C}$ and integrated in microfluidics (a) functionalized with the probe 1, (b) after hybridization with the complementary strand FCT labeled at the 5' with fluorescein, (c) after denaturation at $120\text{ }^\circ\text{C}$ for 5 min, and (d) after rehybridization with FCT. Bars are $150\text{ }\mu\text{m}$.

Zr^{4+} ions very prone to the electrostatic interaction and favors the DNA bonding. In fact, the presence of hydroxide groups on the oxide surface brings the formation of surface electrical charges in aqueous media whose sign is highly pH dependent.^{46,47} By using an acidic solution to develop our ZrO_2 structures ($\text{pH} < \text{isoelectric point, IEP}$), the film surface became positively charged, allowing greater selectively toward phosphorylated molecules.

Nevertheless, the free phosphate group introduced on the 5' end of oligonucleotides needs to dominate over the backbone phosphate diester moieties in binding to Zr ions, in order to lead a right DNA configuration. Two more factors can be considered to explain the specific strong bond of DNA through the 5'-phosphate group: the strand conformation and the acid–base properties. Looking at the oligonucleotides structure, the phosphate functionalities in the backbone are less liable to binding than the terminal phosphate group, due to the steric hindrance. Moreover, as many metal oxides, ZrO_2 acts as a Lewis acid⁴⁸ and acid–base interactions certainly contribute to the different selectivity in oligonucleotides immobilization. The phosphate group of DNA can be divided in two classes: basic and weak or nonbasic phosphates. Disubstituted phosphates along the backbone have a pK_a of around 2 and bear a -1 charge, so they appear to be very weak basic moieties.

Monosubstituted, terminal 5' phosphates with a -2 charge and a pK_a value of around 6–7 are more basic groups.⁴⁵ As consequence, the different acid–base strength induces a more favorable anchoring through the free 5' phosphate end.

Therefore, synthesis conditions (e.g., temperature, pH, and so on) strongly influence the material characteristics: amount and peculiarity of surface acidic sites in Zr metal oxides play a fundamental role in the overall immobilization process. The ZrO_2 system has been thoroughly characterized by FT-IR spectroscopy to better understand the surface chemistry driven anchoring on the ZrO_2 films.

As mentioned, the second important aspect for DNA recognition and sensing applications is reproducibility, that has been evaluated by a multistep experiment (hybridization–denaturation–rehybridization). A phosphorylated probe sol ($1\text{ }\mu\text{M}$) has been put inside the microfluidic channel for 1 h at RT and rinsed with DNase free water to remove the not absorbed ssDNA (Figure 8a). The complementary target FCT (sol $1\text{ }\mu\text{M}$), labeled in 5' with fluorescein, has been incubated inside the channel for 30 min in the dark. Afterward, the sample had been washed and analyzed under the fluorescence microscope.

Figure 8b clearly shows that the hybridization occurred just inside the channel and onto the patterned features, confirming the selective immobilization of oligonucleotides in these areas.

The microfluidic platform has been heated at a temperature higher than 120 °C for 5 min after the hybridization in order to check the stability of the system and the reproducibility of the recognition event. In this condition, DNA undergoes denaturation: the separation of a double strand into two single ones occurs thanks to the temperature induced breaking of hydrogen bonds between the bases. After channel washing with DNase free water, the complete removal of fluorescently labeled target seems to be successful. The signal intensity inside and outside the channel is the same (Figure 8c), indicating a complete regeneration of the surface.

The reliability of probe anchoring has also been checked by a new complementary target FCT incubation, applying the previously described protocol. The final outcome is reported in Figure 8d, showing the fluorescence appearance on ZrO₂ structures inside the channel. The probe has been retained even after the annealing and the biological activity is demonstrated. The anchoring of phosphate compounds on the zirconium oxide surface first proceeds by a reversible noncovalent interaction with the adsorbed H₂O, OH, and oxo groups covering the surface, followed by formation of strong highly covalent bonds resulting from the displacement of oxo and hydroxyl groups by the phosphate oxygen atoms.²⁷ This mechanism can explain the stability of interaction between the phosphorylated groups and the ZrO₂ surface.

The preservation of bond between the probe 5' phosphate group and ZrO₂ regions confirms the viability of the proposed material as an advanced platform for DNA positioning and detection of DNA hybridization. Moreover, the successful denaturation and the possibility for surface recovery is an important point in sensing applications.

CONCLUSIONS

A new platform for spatially controlled and oriented immobilization of oligonucleotides in the microfluidic architecture has been engineered. A simple functionalization protocol for DNA anchoring has been achieved by using a photosensitive interface based on a ZrO₂ sol-gel system. Exploiting the ability of sol-gel materials to be easily deposited on several substrates (glass, silicon, gold, and so on), this approach allows one to keep the same anchoring procedure for all of them and overcome some time-consuming and multistep protocols typical of these commonly used substrates. Crystalline directly patterned ZrO₂ microstructures have been easily integrated in the microfluidic channel, using conventional sealing techniques. The annealing process, used to crystallize ZrO₂ and to maximize DNA affinity, does not affect the pattern shape: the lateral dimension of the features is maintained.

Biofunctionalization and hybridization tests made directly in the microfluidic channels show that DNA selectively anchors to the patterned zirconium oxide areas without any modification, through a naturally occurring 5' terminal phosphate and preserving biological activity. Moreover, bioactivity reliability of the system has been demonstrated through hybridization-denaturation-rehybridization experiments. The overall strategy provides an easy way to endow microfluidic structures with additional functionalities and can find potential application in many challenging fields such as biomolecular enrichment, separation, sensing, microarray for transcriptional analysis, and immunoassay.

ASSOCIATED CONTENT

Supporting Information

Spin curves, bonding test, surface activation, melting point of ssDNA strands, and nonspecific absorption tests. The Supporting Information is available free of charge on the ACS Publications website at DOI: 10.1021/acsami.5b01058.

AUTHOR INFORMATION

Corresponding Author

*E-mail: giovanna.brusatin@unipd.it. Phone: +39 0498275723. Fax: +39 0498275505.

Author Contributions

G.D.G. and G.B. wrote the manuscript. G.D.G. synthesized the photosensitive material, realized patterned zirconia samples, and performed the pertaining characterization measurements. A.Z. and F.L. performed microfluidic integration and DNA binding. N.E. and G.B. supervised the research. All authors have given approval to the final version of the manuscript.

Notes

The authors declare no competing financial interest.

ACKNOWLEDGMENTS

Fondazione Cariplo is greatly acknowledged for the financial support through the Project No. 2012-0186.

REFERENCES

- (1) Ramsay, G. DNA Chips: State-of-the Art. *Nat. Biotechnol.* **1998**, *16*, 40–44.
- (2) Zhou, X. C.; Huang, L. Q.; Yau Li, S. F. Microgravimetric DNA Sensor Based on Quartz Crystal Microbalance: Comparison of Oligonucleotide Immobilization Methods and the Application in Genetic Diagnosis. *Biosens. Bioelectron.* **2001**, *16*, 85–95.
- (3) Heise, C.; Bier, F. F. Immobilization of DNA on Microarrays. *Top. Curr. Chem.* **2005**, *261*, 1–25.
- (4) Fahrenkopf, N. M.; Shahedipour-Sandvik, F.; Tokranova, N.; Bergkvist, M.; Cady, N. C. Direct Attachment of DNA to Semiconducting Surfaces for Biosensor Applications. *J. Biotechnol.* **2010**, *150*, 312–314.
- (5) Hoheisel, J. D. Microarray Technology: Beyond Transcript Profiling and Genotype Analysis. *Nature* **2006**, *7*, 200.
- (6) Liu, B.; Liu, J. DNA Adsorption by Magnetic Iron Oxide Nanoparticles and Its Application for Arsenate Detection. *Chem. Commun.* **2014**, *50*, 8568–8570.
- (7) Nonglaton, G.; Benitez, I. O.; Guisle, I.; Pipelier, M.; Léger, J.; Dubreuil, D.; Tellier, C.; Talham, D. R.; Bujoli, B. New Approach to Oligonucleotide Microarrays Using Zirconium Phosphonate-Modified Surfaces. *J. Am. Chem. Soc.* **2004**, *126* (5), 1497–1502.
- (8) Mohanty, S. P.; Kougiannos, E. Biosensors: A Tutorial Review. *IEEE Potentials* **2006**, *2*, 35–40.
- (9) Dutse, S. W.; Yusof, N. A. Microfluidics-Based Lab-on-Chip Systems in DNA-Based Biosensing: An Overview. *Sensors* **2011**, *11*, 5754–5768.
- (10) Choi, S.; Goryll, M.; Mandy Sin, L.-Y.; Wong, P. K.; Chae, J. Microfluidic-Based Biosensors Toward Point-of-Care Detection of Nucleic Acids and Proteins. *Microfluid. Nanofluid.* **2011**, *10*, 231–247.
- (11) Kim, J.H.-S.; Marafie, A.; Jia, X.-Y.; Zoval, J. V.; Madou, M. J. Characterization of DNA Hybridization Kinetics in a Microfluidic Flow Channel. *Sens. Actuators, B* **2006**, *113*, 281–289.
- (12) Pappaert, K.; Van Hummelen, P.; Vanderhoeven, J.; Baron, G. V.; Desmet, G. Diffusion-Reaction Modelling of DNA Hybridization Kinetics on Biochips. *Chem. Eng. Sci.* **2003**, *58*, 4921–4930.
- (13) Solomun, T.; Mix, R.; Sturm, H. Immobilization of Silanized DNA on Glass: Influence of the Silane Tether on the DNA Hybridization. *ACS Appl. Mater. Interfaces* **2010**, *2*, 2171–2174.

- (14) Strother, T.; Cai, W.; Zhao, X.; Hamers, R. J.; Smith, L. M. Synthesis and Characterization of DNA-Modified Silicon (111) Surfaces. *J. Am. Chem. Soc.* **2000**, *122*, 1205–1209.
- (15) Taylor, S.; Smith, S.; Windle, B.; Guiseppi-Elie, A. Impact of Surface Chemistry and Blocking Strategies on DNA Microarrays. *Nucleic Acids Res.* **2003**, *31*, No. e87.
- (16) Brassard, D.; Clime, L.; Li, K.; Geissler, M.; Miville-Godin, C.; Roy, E.; Veres, T. 3D Thermoplastic Elastomer Microfluidic Devices for Biological Probe Immobilization. *Lab Chip* **2011**, *11*, 4099.
- (17) Suzuki, Y.; Yamada, M.; Seki, M. Sol–Gel Based Fabrication of Hybrid Microfluidic Devices Composed of PDMS and Thermoplastic Substrates. *Sens. Actuators, B* **2010**, *148*, 323–329.
- (18) Yin, H. B.; Brown, T.; Wilkinson, J. S.; Eason, R. W.; Melvin, T. Submicron Patterning of DNA Oligonucleotides on Silicon. *Nucleic Acids Res.* **2004**, *32*, No. e118.
- (19) Banuls, M.-J.; Puchades, R.; Maquieira, A. Site-Specific Immobilization of DNA on Silicon Surfaces by Using the Thiol–yne Reaction. *J. Mater. Chem. B* **2014**, *2*, 8510–8517.
- (20) Fiddes, L. K.; Chan, H. K. C.; Lau, B.; Kumacheva, E.; Wheeler, A. R. Durable, Region-Specific Protein Patterning in Microfluidic Channels. *Biomaterials* **2010**, *31*, 315–320.
- (21) Ruiz, S. A.; Chen, C. S. Microcontact Printing: A Tool to Pattern. *Soft Matter* **2007**, *3*, 1–11.
- (22) Didar, T. F.; Foudeh, A. M.; Tabrizian, M. Patterning Multiplex Protein Microarrays in a Single Microfluidic Channel. *Anal. Chem.* **2012**, *84*, 1012–1018.
- (23) Demers, L. M.; Ginger, D. S.; Park, S.-J.; Li, Z.; Chung, S.-W.; Mirkin, C. A. Direct Patterning of Modified Oligonucleotides on Metals and Insulators by Dip-Pen Nanolithography. *Science* **2002**, *296*, 1836–1838.
- (24) Perl, A.; Reinhoudt, D. N.; Huskens, J. Microcontact Printing: Limitations and Achievements. *Adv. Mater.* **2009**, *21*, 2257–2268.
- (25) Braunschweig, A. B.; Senesi, A. J.; Mirkin, C. A. Redox-Activating Dip-Pen Nanolithography (RA-DPN). *J. Am. Chem. Soc.* **2009**, *131*, 922–923.
- (26) Xiao, W.; Huang, J. Immobilization of Oligonucleotides onto Zirconia-Modified Filter Paper and Specific Molecular Recognition. *Langmuir* **2011**, *27*, 12284–12288.
- (27) Cinier, M.; Petit, M.; Pecorari, F.; Talham, D. R.; Bujoli, B.; Tellier, C. Engineering of a Phosphorylatable Tag for Specific Protein Binding on Zirconium Phosphonate Based Microarrays. *J. Biol. Inorg. Chem.* **2012**, *17*, 399–407.
- (28) Singh, V.; Zharnikov, M.; Gulinoc, A.; Gupta, T. DNA Immobilization, Delivery and Cleavage on Solid Supports. *J. Mater. Chem.* **2011**, *21*, 10602–10618.
- (29) Hussain, S. A.; Paul, P. K.; Dey, D.; Bhattacharjee, D.; Sinha, S. Immobilization of Single Strand DNA on Solid Substrate. *Chem. Phys. Lett.* **2007**, *450*, 49–54.
- (30) Meyer, R.; Giselbrecht, S.; Rapp, B. E.; Hirtz, M.; Niemeyer, C. M. Advances in DNA-Directed Immobilization. *Curr. Opin. Chem. Biol.* **2014**, *18*, 8–15.
- (31) Linford, M. R.; Chidsey, C. E. D. Alkyl Monolayers on Silicon Prepared from 1-Alkenes and Hydrogen-Terminated Silicon. *J. Am. Chem. Soc.* **1995**, *117*, 3145–3152.
- (32) Li, F.; Chen, W.; Zhang, S. Development of DNA Electrochemical Biosensor Based on Covalent Immobilization of Probe DNA by Direct Coupling of Sol-Gel and Self-Assembly Technologies. *Biosens. Bioelectron.* **2008**, *24* (4), 787–792.
- (33) Ganguly, A.; Chen, C. P.; Lai, Y. T.; Kuo, C. C.; Hsu, C. W.; Chen, K. H.; Chen, L. C. Functionalized GaN Nanowire-Based Electrode for Direct Label-Free Voltammetric Detection of DNA Hybridization. *J. Mater. Chem.* **2009**, *19*, 928–933.
- (34) Jin, W.; Lin, X.; Lv, S.; Zhang, Y.; Jin, Q.; Mu, Y. A DNA Sensor Based on Surface Plasmon Resonance for Apoptosis-Associated Genes Detection. *Biosens. Bioelectron.* **2009**, *24* (5), 1266–1269.
- (35) Shankaran, D. R.; Gobi, K. V.; Miura, N. Recent Advancements in Surface Plasmon Resonance Immunosensors for Detection of Small Molecules of Biomedical, Food and Environmental Interest. *Sens. Actuators, B* **2007**, *121*, 158–177.
- (36) Monot, J.; Petit, M.; Lane, S. M.; Guisle, I.; Léger, J.; Tellier, C.; Talham, D. R.; Bujoli, B. Towards Zirconium Phosphonate-Based Microarrays for Probing DNA-Protein Interactions: Critical Influence of the Location of the Probe Anchoring Groups. *J. Am. Chem. Soc.* **2008**, *130*, 6243–6251.
- (37) Bujoli, B.; Lane, S. M.; Nonglaton, G.; Pipelier, M.; Léger, J.; Talham, D. R.; Tellier, C. Metal Phosphonates Applied to Biotechnologies: A Novel Approach to Oligonucleotide Microarrays. *Chem.—Eur. J.* **2005**, *11*, 1980–1988.
- (38) Della Giustina, G.; Garoli, D.; Romanato, F.; Brusatin, G. Zirconia Based Functional Sol-Gel Resist for UV and High Resolution Lithography. *Microelectron. Eng.* **2013**, *110*, 436–440.
- (39) Zambon, A.; Zoso, A.; Luni, C.; Frommer, W. B.; Elvassore, N. Determination of Glucose Flux in Live Myoblasts by Microfluidic Nanosensing and Mathematical Modeling. *Integr. Biol.* **2014**, *6*, 277–288.
- (40) Aguilar, D. H.; Torres-Gonzalez, L. C.; Torres-Martinez, L. M.; Lopez, T.; Quintana, P. A Study of the Crystallization of ZrO₂ in the Sol-Gel System: ZrO₂-SiO₂. *J. Solid State Chem.* **2000**, *158*, 349–357.
- (41) Fahrenkopf, N. M.; Rice, P. Z.; Bergkvist, M.; Deskins, N. A.; Cady, N. C. Immobilization Mechanisms of Deoxyribonucleic Acid (DNA) to Hafnium Dioxide (HfO₂) Surfaces for Biosensing Applications. *ACS Appl. Mater. Interfaces* **2012**, *4*, 5360–5368.
- (42) Leitner, A. Phosphopeptide Enrichment Using Metal Oxide Affinity Chromatography. *Trends Anal. Chem.* **2010**, *29*, 177–185.
- (43) Choi, S.; Chae, J. Methods of Reducing Non-Specific Adsorption in Microfluidic Biosensors. *J. Micromech. Microeng.* **2010**, *20*, 075015.
- (44) Wolf, L. K.; Gao, Y.; Georgiadis, R. M. Sequence-Dependent DNA Immobilization: Specific versus Nonspecific Contributions. *Langmuir* **2004**, *20*, 3357–3361.
- (45) Liu, J. Adsorption of DNA onto Gold Nanoparticles and Graphene Oxide: Surface Science and Applications. *Phys. Chem. Chem. Phys.* **2012**, *14*, 10485–10496.
- (46) Degen, A.; Kosec, M. Effect of pH and Impurities on the Surface Charge of Zinc Oxide in Aqueous Solution. *J. Eur. Ceram. Soc.* **2000**, *20*, 667–673.
- (47) Wei, W. C. J.; Wang, S. C.; Ho, F. Y. Electrokinetic Properties of Colloidal Zirconia Powders in Aqueous Suspension. *J. Am. Ceram. Soc.* **1999**, *82*, 3385–3392.
- (48) Jeong, N. C.; Lee, J. S.; Tae, E. L.; Lee, Y. J.; Yoon, K. B. Acidity Scale for Metal Oxides and Sanderson's Electronegativities of Lanthanide Elements. *Angew. Chem., Int. Ed.* **2008**, *47*, 10128–10132.